PROCEEDINGS, Twenty-Eighth Workshop on Geothermal Reservoir Engineering
Stanford University, Stanford, California, January 27-29, 2003
SGP-TR-173

LARGE-SCALE PHYSICAL MODELING OF WATER INJECTION INTO GEOTHERMAL RESERVOIRS AND CORRELATION TO SELF POTENTIAL MEASUREMENTS

Jeffrey R. Moore, Steven D. Glaser, and H. Frank Morrison

University of California, Berkeley
440 Davis Hall
Berkeley, CA 94720, USA
e-mail: moore@ce.berkeley.edu

ABSTRACT

Laboratory measurements of electric self potentials resulting from water injection through a known flow path in a 260 mm cube of Nugget sandstone are used to calibrate a new large-scale testing device that simulates the in-situ conditions at an injection point in a geothermal reservoir. Modeled in-situ temperatures were 20°C and 150°C, while injection pressures were varied from 1 to 1200 kPa. The observed self potential response showed an accurate spatial correlation to the known flow path, with potential differences on the order of 100 mV. A surface contour map of potentials was generated for the sample cube, and the temporal variation of potentials with injection pressure shows good correlation. Results suggest that at higher temperatures, and in the presence of steam, opposing electrokinetic and thermoelectric self potentials, combined with decreased sample resistivity, may counteract to lower the observed potential on the sample surface. Incomplete saturation of the sample at low temperature may produce capacitive effects among the mineral grains leading to a slow decay in observed potentials following the end of injection. A second testing program on Berea sandstone cores at room temperature reinforces these results. This four-part program isolated the effects of the intact rock, the empty flow pipe, the sand–filled flow pipe, and the quartz sand alone. Streaming potential coupling coefficients for the intact core, the core with empty flow pipe, and the core with sand-filled flow pipe are observed to be approximately constant over a large pressure difference range (up to 1.2 MPa), and are 42 mV/atm, -10 mV/atm, and 42 mV/atm respectively. The coupling coefficient for the test of only coarse quartz sand revealed a logarithmically decreasing coupling coefficient that varied from 60 mV/atm at low pressures to 32 mV/atm at 300 kPa. This testing showed excellent correlation between applied pressure drop and observed streaming potential, and indicates the ability of streaming potentials to identify changes in sample conditions.

INTRODUCTION

Self-potential, in this case streaming potential (or electrokinetic potential), is a widely recognized method for identifying flow paths through rock and rock/soil matrices (Bogoslovsky and Ogilvy, 1970; Corwin and Hoover, 1979; Wurmstich and Morgan, 1994). This method is based on the existence of an electric double layer at the liquid-matrix interface where a diffuse mobile layer of ions can be effectively *dragged* away from their adsorbed immobile counterparts under a pore pressure gradient, creating a charge imbalance (Jouniax et al, 1999). Since many minerals have negatively charged surfaces, a diffuse layer of positive ions from the local pore solution weakly bonds to the surface, and can be carried away from the mineral surface yielding a negative anomaly. Areas where water collects (for the above case) would be then characterized by a collection of positive charges, and a positive anomaly (Vichabian and Morgan, 2002).

The Helmholtz-Smoluchowski equation describes the relationship between streaming potentials and the pressure gradient under which they move.

$$\Delta V = (\varepsilon\zeta / \mu\sigma)\, \Delta P \qquad (1)$$

Where ε is the dielectric constant of the fluid, ζ is the zeta potential, σ is the conductivity of the fluid, and μ is the fluid viscosity (Overbeek, 1952). The quantity $(\varepsilon\zeta/\mu\sigma)$ is known as the streaming potential coupling coefficient, Cc.

Precise quantitative interpretation of streaming potential data can sometimes be difficult, as the coupling coefficient must be previously determined for each specific scenario. Many users of the streaming potential method have relied on a qualitative interpretation of data in which fluid flow paths are identified by contouring data collected on a dense grid of electrodes. Such methodology has been successfully applied to many field problems, most notably the detection of flow paths through earth

dams (Ogilvy et al, 1969; Johansson, et al, 2000), and more relevantly, flow detection resulting from hydraulic stimulation of hot dry rock (or enhanced geothermal systems) reservoirs (Kawakami and Takasugi, 1994; Marquis et al, 2002).

We analyze the temporal response of the induced potentials, and its relationship with injection pressure. Furthermore, we investigate effects of another type of self potential, the thermoelectric potential, which is a result of a temperature gradient and is commonly observed in active geothermal areas (Corwin and Hoover, 1979).

The results presented have been obtained as calibration experiments for large-scale physical testing to investigate damage mechanisms at injection points in geothermal reservoirs. Calibration of the streaming potential response for a known flow path will aid in the interpretation of data for an unknown, possibly chaotic and temporally variable, natural flow path. Temperature effects were modeled by varying sample temperature from 20° C to 150° C. The effect of variations in injection pressure and rate were also analyzed with respect to the observed geophysical response.

EXPERIMENTAL SETUP

Testing is subdivided into 2 programs. The first testing program involves large-scale tests on a 260 mm cube of Nugget sandstone. Streaming potential tests were performed for 2 different sample conditions: 1) water-filled, room temperature sample, and 2) steam-saturated, 150°C sample. The next testing program was designed to isolate certain mechanisms observed in the large-scale testing, and involves the use of a 127 mm long, 25 mm diameter core of Berea sandstone. This testing program has 4 subdivisions: a) intact core, b) core with 5 mm diameter empty hole along cylinder axis, c) core with hole filled with coarse quartz sand, and d) quartz sand only. Each of these tests reveals information which will aid in the interpretation of data from the large-scale test.

Large-Scale Triaxial Testing – Nugget Sandstone

The testing device (Figure 1) is a true-triaxial cell containing a 260 mm cubic sample of Nugget Sandstone (American Stone, Salt Lake City, Utah). It is capable of 3 independent confining pressures up to 14 MPa, while being flooded by up to 250° C steam. The sample is surrounded by non-conductive PEEK plastic plates, which have a dense grid of machined grooves to allow for unimpeded movement of steam and condensate around the sample. Fifty non-polarizing copper electrodes are attached to these plates, distributed on all sides of the sample at 70 mm spacing. Four 2000 Watt heater coils are embedded in aluminum plates outside the PEEK plates, which can be used simultaneously with the steam to apply superheat, or independently, as in modeling a hot dry rock (or EGS) system. Steam (57 kg/hr) is produced in a Lattner 480 V, 2 MPa electric boiler fed by pre-heated water.

The injection pump was created by coupling a hydraulic cylinder to a variable speed actuator. The hydraulic cylinder has a 76 mm bore and a 305 mm stroke, and is made from brass to resist corrosion. The hydraulic actuator has a 350 mm stroke and is driven by a variable frequency motor controller operating from 0 to 60Hz. Injection rates up to 50 cc/sec are possible at pressures up 14 MPa. Injection rate is controlled either manually by a speed potentiometer, or by control loop feedback from the position sensor attached to the hydraulic actuator.

Figure 1: Triaxial testing device including (from left to right) data acquisition digitizer, injection pump, true-triaxial cell, and air/hydraulic intensifiers. Boiler is in background behind injector.

The calibration model was created by drilling two intersecting holes in the sample interior. One hole was 9.5 mm diameter and extended from the center of the top face of the sample to a depth of ½ the sample height. This hole housed the self-sealing injector. The other hole was 5 mm diameter and extended radial from the base of the main hole out to the center of one side face forming an 'L' (Figure 2). This hole was packed with coarse quartz sand (masonry sand). Water injected at the center of the sample traveled through the intersecting sand-filled hole horizontally towards the block edge. The surrounding PEEK plastic plate at the sample face was machined to allow this injectate to escape around the block perimeter. Confining stress was held at a constant 1 MPa in all three principle directions in order to minimize the contact resistance of the electrodes. The reference electrode for all testing was located at the center of the sample (Figure 2). The sampling rate was 200 samples per second for 80 second sweeps.

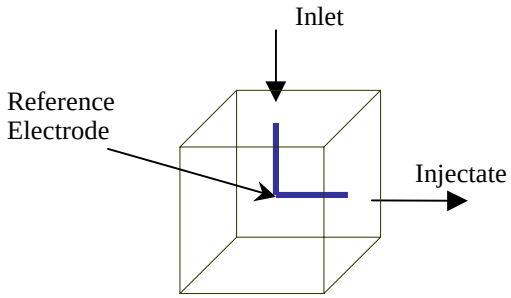

Figure 2: Schematic of artificial flow path

This testing configuration has been specifically designed to model the realistic condition of piped flow in a conducting rock matrix. Many previous laboratory measurements have neglected conducting boundaries, opting in the interest of simplicity for samples contained within a glass or plastic tube. The effect of conducting walls of the pipe will be to allow a portion of the induced current to flow through the rock matrix, while a portion flows in the pipe. We believe that this testing set-up provides a more realistic, and therefore useful, set of results for application to real-world problems.

Small-Scale Core Testing – Berea Sandstone

This testing device was constructed to hold a 127 mm long core of 25 mm diameter Berea sandstone (Lang Stone, Columbus, Ohio). The device (Figure 3) was made using clear PVC pipe and 2 end flanges, to which were attached 100 mm square Plexiglas end plates. The sample was coated with silicon adhesive prior to being inserted into the pipe to ensure that there was no flow allowed at the sample/pipe interface. A copper screw at each end was used as an electrode and threaded through the end plates so that it could be tightened against the sample to ensure good contact. A perforated stainless steel cover protected against accidental breakage, as well as isolated the sample from stray electrical noise.

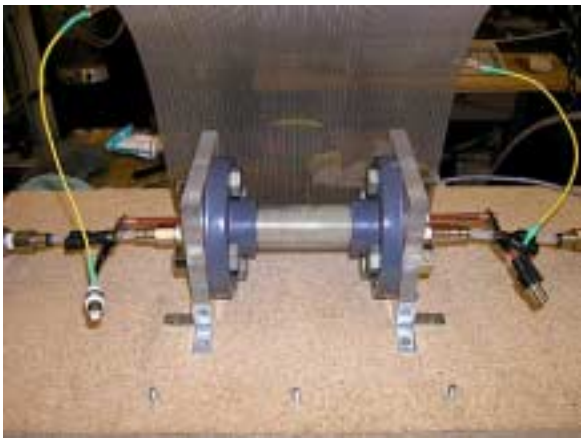

Figure 3: Core sample testing device with Berea sandstone. Core is 127 mm long and 25 mm diameter. Copper screws are electrodes.

Water was applied to the sample by each of two methods. First, a static head method was employed where a large container of water was placed at different elevations above the sample, and the head difference measured. The maximum attainable pressure drop using this method was 30 kPa. Second, the injection pump previously described applied water to the sample at pressures up to 1300. All injectate was 200 Ohm-m tap water.

RESULTS

Large-Scale Triaxial Testing – Nugget Sandstone

Testing for this sample configuration was done at both low and high temperatures. The low-temperature sample was at 20°C. For high-temperature samples, the rock was flooded with steam produced in a boiler to bring it to 150°C. Streaming potentials were generated by applying injectate via the injection pump, and this applied pressure measured. The spatial orientation of observed potentials, as well as the temporal variations of potentials and injection pressure was noted. Streaming potential coupling coefficients were not determined in this testing program because the pressure at the outlet of the sand-filled flow pipe was unknown.

Low Temperature – Water Filled

Testing on 260 mm cubic sample of Nugget sandstone was first investigated at room temperature, or about 20°C. Testing included injections at various pressures and flow rates. Streaming potential measurements were made spatially on each of the 4 sides of the block perimeter (neglecting the top and bottom faces). Spatial variations in streaming potentials resulting from a 275 kPa injection are shown contoured in Figure 4. These results are typical of the 100 or so injections performed. Recall that the flow direction is towards the *east* face. The location of the outlet pipe is marked with an X on the *east* face, and the observed streaming potentials accurately define the spatial orientation of this outlet. For the other side faces, observed potentials showed a ~25 mV drop with only slight spatial variation. This variation, however, weakly defined the flow orientation within the sand-filled pipe, which is denoted by the arrows on the contour plot.

Figure 5 illustrates the temporal variation of streaming potentials with injection pressure for the electrode nearest the flow pipe outlet. The observed potentials and the applied pressure showed good correlation. For all testing, streaming potentials responded well to increasing head, mimicking the pressure increase, while for decreasing head experiments, potentials were observed to decay slowly following the decreasing in pressure.

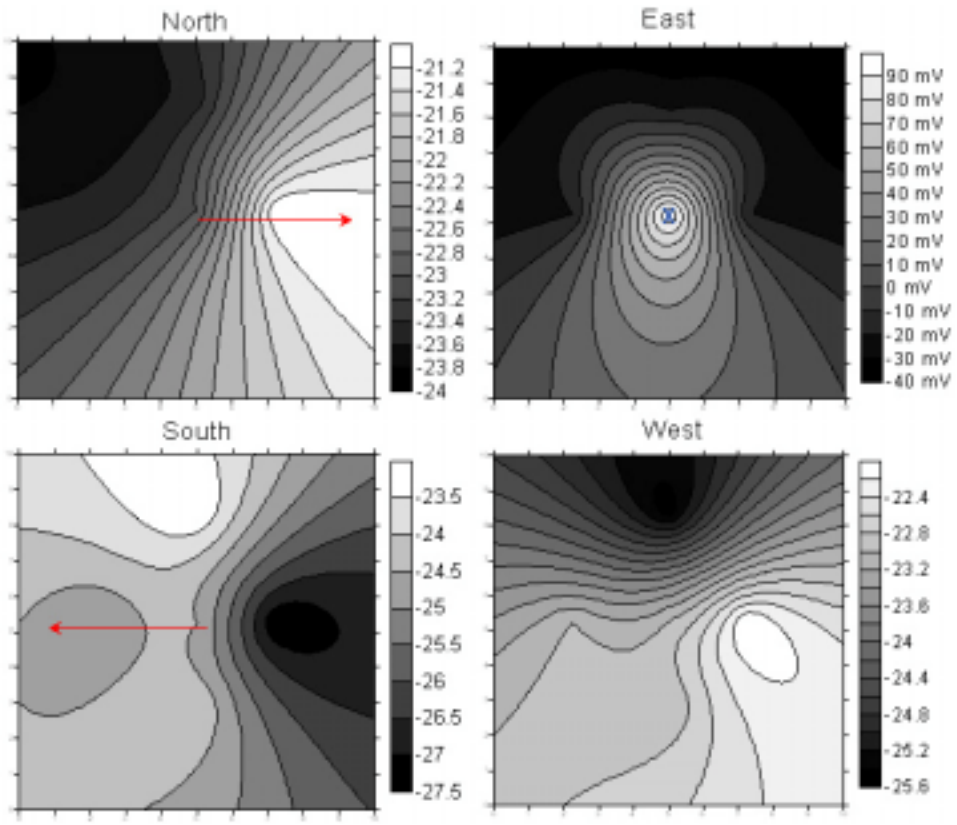

Figure 4: Contoured spatial variation of streaming potentials over the sample surface for large-scale sample at 20°C. Flow is towards the *east* face and the outlet of the flow pipe is indicated by an X. Values taken at 40 seconds time.

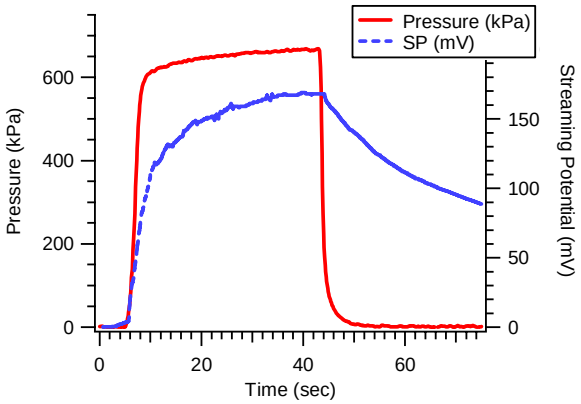

Figure 5: Injection pressure and streaming potential temporal response for large-scale sample at 20°C for electrode nearest the flow pipe outlet.

High Temperature – Steam Saturated

The sample was brought to 150°C at 400 kPa pore pressure by applying steam produced in a boiler. The steam-saturated sample was then subjected to the same testing program as the low-temperature sample. Spatial variations in streaming potentials resulting from a 500 kPa injection are illustrated in Figure 6. Again, the variations in potentials accurately define the spatial orientation of the sand-filled flow pipe. For the other side faces, observed potentials showed a ~230 mV drop with only slight spatial variation. The large magnitude of this drop as compared to the cool sample indicates that there may be additional mechanisms contributing the observed potentials. A hypothesis to this end will follow.

For the high-temperature sample, observed peak potentials were actually lower in magnitude for the high-temperature sample than the low-temperature sample. This result is in contradiction to Morgan et al (1989) and others who predicted that two-phase flow may enhance streaming potentials by up to 4 times. We will discuss a hypothesis that competing effects may interact to produce lower potentials.

The temporal variation of streaming potential and applied pressure showed a relationship different than that for the cold sample. While the streaming potential response reacted well to the beginning of injection, it began to decline shortly thereafter and continued to decline then rise as injection progressed (Figure 7). It is clear from this complicated response that there are many mechanisms contributing to observed potentials. To investigate these mechanisms, the second testing program was employed.

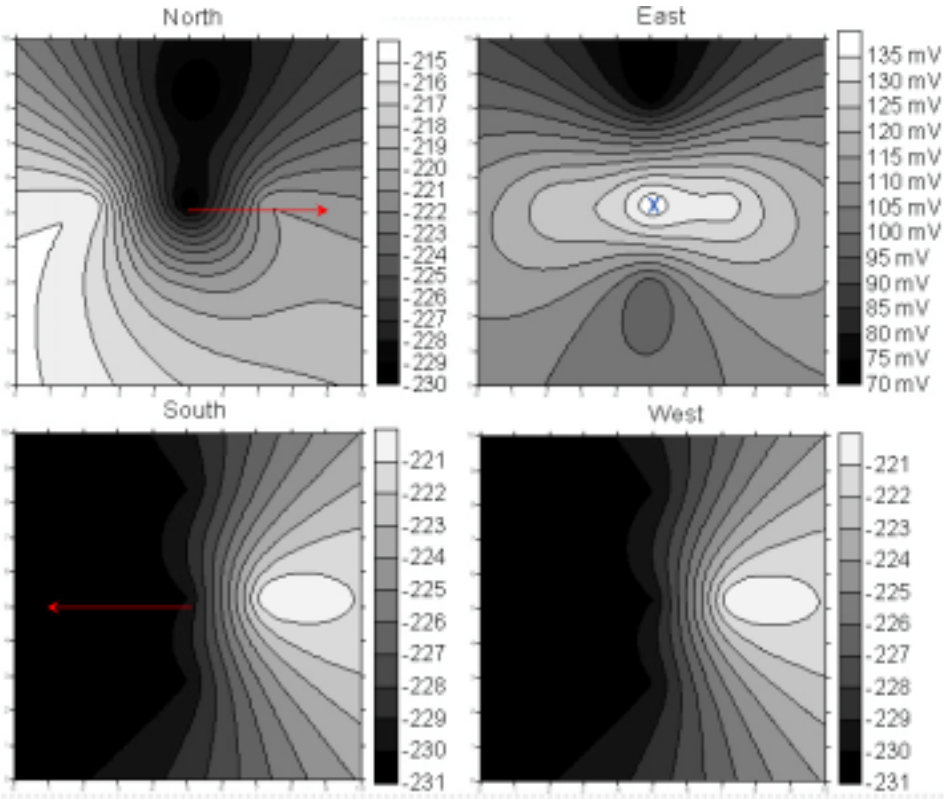

Figure 6: Contoured spatial variation of streaming potentials over the sample surface for large-scale, steam-saturated sample at 150°C. Flow is towards the *east* face and the outlet of the flow pipe is indicated by an X. Readings taken at 42 seconds time.

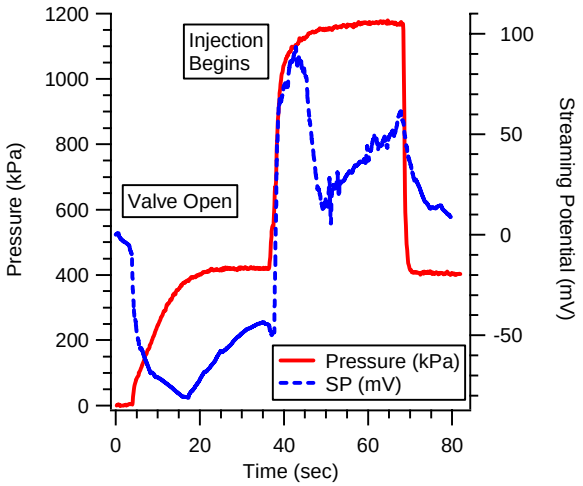

Figure 7: Injection pressure and streaming potential temporal response for large-scale steam-saturated sample at 150°C. Electrode location is that nearest the flow pipe outlet.

Small-Scale Core Testing – Berea Sandstone

This testing in this program had 4 stages designed to isolate the mechanisms contributing to the streaming potential response observed in the large-scale testing. Stage #1 included streaming potential investigations for a 127 mm long, 25 mm diameter intact core of Berea sandstone. For stage #2, a 5 mm diameter hole was drilled down the axis of the core and its effect investigated. In stage #3, this hole was filled with coarse quartz sand, and streaming potential variation with pressure difference explored. Stage #4 investigated streaming potentials generated in a sample of the coarse sand only. Central to this investigation was determining the streaming potential coupling coefficient (Cc) for each stage.

Coupling Coefficient

For the intact core of Berea Sandstone, the streaming potential coupling coefficient was determined to be about 45 mV/atm. This value was constant over a pressure drop range of 1 to 600 kPa. Figures 8 and 9 illustrate both static head experiments at low pressures, and higher-pressure experiments using the injection pump. These figures illustrate that the coupling coefficient is constant over the large pressure range tested.

For the core sample of Berea sandstone with a 5 mm diameter hole drilled down its axis, static head experiments revealed that the coupling coefficient was –10 mV/atm. Accordingly, potential differences generated were quite low. Figure 10 illustrates this result. For this setup, trials using the injection pump were inconclusive because it was difficult to generate a significant head loss over the sample.

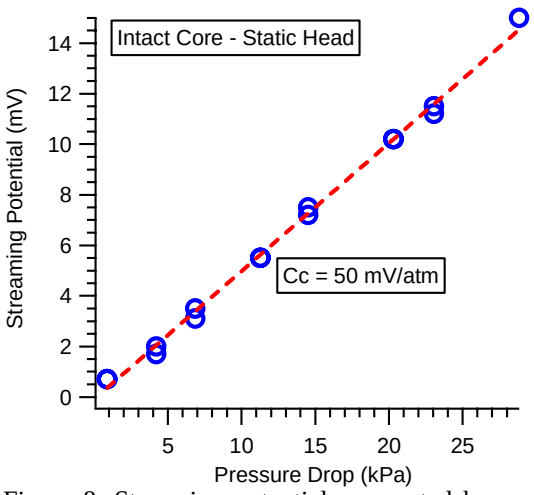

Figure 8: Streaming potentials generated by various pressure drops for the intact core test using the static head method.

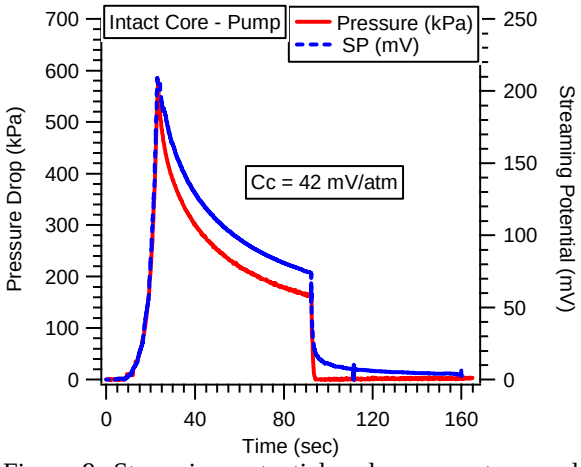

Figure 9: Streaming potential and pressure temporal response for the intact core. Coupling coefficient is determined by overlaying curves.

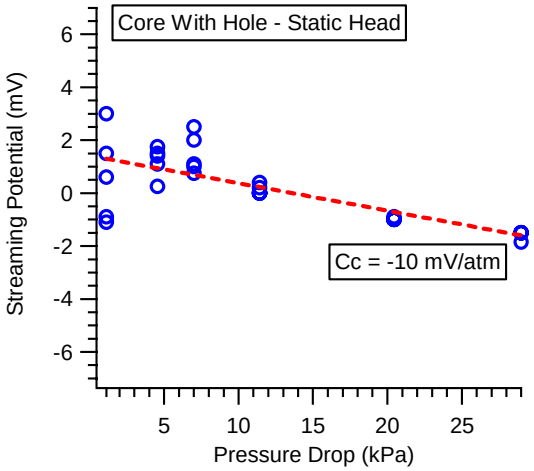

Figure 10: Streaming potentials generated by various pressure drops for the core with empty hole test using the static head method.

The next test performed was a sample of coarse quartz sand only, the same as filled the pipe in the large-scale test sample. For this sand-only sample, the coupling coefficient was observed to vary inversely with the pressure drop across the sample. This variation is described by equation (2) for injection pressures above 75 kPa, and is illustrated in Figures 11 and 12.

$$Cc = -8 \ln (\Delta P) + 80 \qquad (2)$$

At pressures less than 75 kPa the coupling coefficient was constant at 50 mV/atm. Coupling coefficient values at higher pressures (300 kPa) were smaller than those at low pressures by nearly half. These results are consistent with observations reported by Morgan et al (1989) that at high pressures the coupling coefficient decreases in magnitude by 2-4 times.

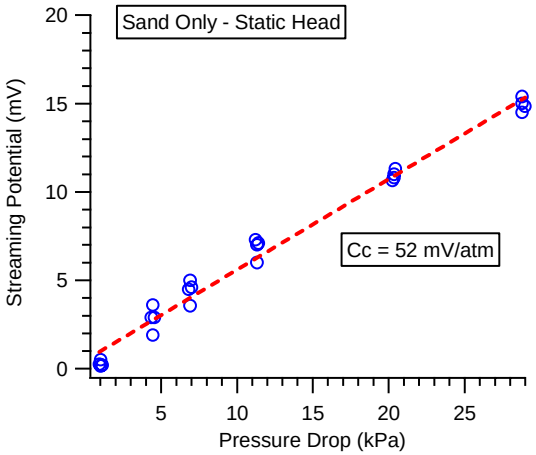

Figure 11: Streaming potentials generated by various pressure drops for the quartz sand test using the static head method.

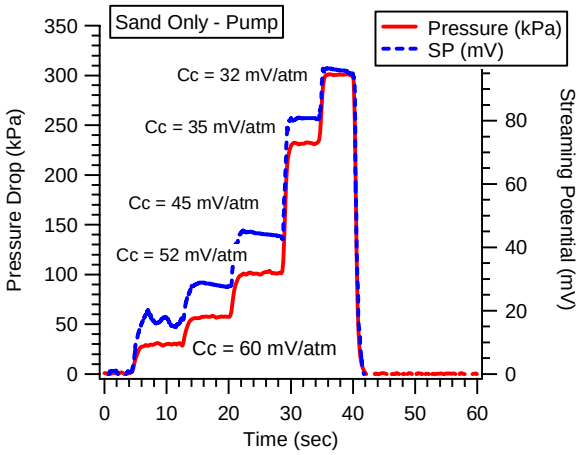

Figure 12: Streaming potential and pressure temporal response for the quartz sand test. Coupling coefficients are determined by overlaying curves. Increasing pressure levels allows for the quantification of changes in coupling coefficient with pressure drop. Coupling coefficient decreased with increasing pressure drop across the sample.

The fourth and final testing configuration was the Berea sandstone core with a 5 mm diameter axial drill hole filled with the coarse quartz sand. This configuration mimics that of the large-scale triaxial testing. For this configuration a coupling coefficient of 42 mV/atm was observed to be approximately constant over a large pressure difference range. Figure 13 shows the results of low-pressure static head testing for this sample, while Figure 14 shows the high-pressure injection pump testing results. The pressure range of testing was from 1-1125 kPa, and the streaming potential coupling coefficient was observed to be constant over this range.

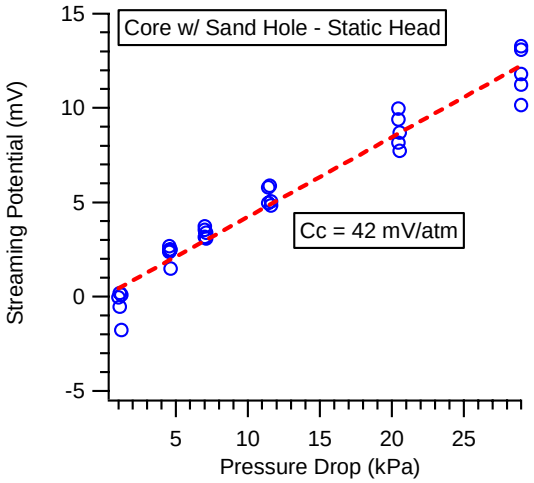

Figure 13: Streaming potentials generated by various pressure drops for the sand-filled pipe test using the static head method.

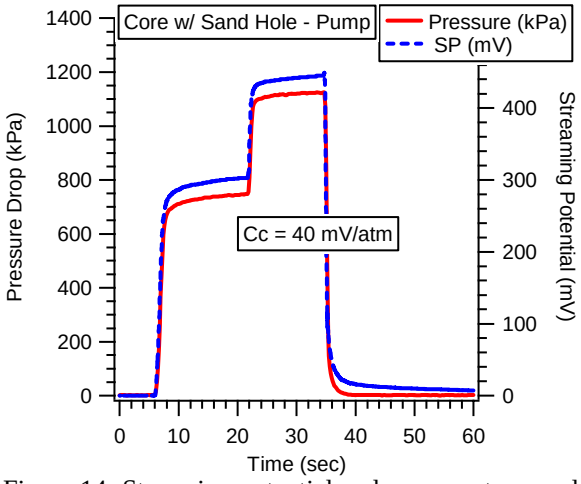

Figure 14: Streaming potential and pressure temporal response for the quartz sand test. Coupling coefficients are determined by overlaying curves. Increasing pressure levels shows no change in coupling coefficient with pressure drop.

Table 1 summarizes the coupling coefficient results from the Berea sandstone streaming potential testing.

Stage	Cc Range	Cc Average
1. Intact	42 – 50 mV/atm	45 mV/atm
2. Core w/ hole	-10 mV/atm	-10 mV/atm
3. Core w/ sand hole	40 - 42 mV/atm	41 mV/atm
4. Sand only	32 – 60 mV/atm	50 mV/atm

DISCUSSION

Large-Scale Triaxial Testing – Nugget Sandstone

Low Temperature – Water Filled

In general, streaming potentials responded well to increasing head, mimicking changes in pressure gradient. For decreasing head, however, potentials were observed to decay slowly following the decrease in pressure. This observation is attributed to capacitive effects of the sample caused by incomplete saturation. Currents induced by the charge imbalance in the flow pipe move through the pore fluid and into the rock matrix. If some portion of the rock pore space is filled with air, then mineral grains can act as capacitors, retaining and slowly releasing current. The slow decay was not observed for the Berea sandstone sample core (see Figure 5), which was more likely to be saturated than the Nugget sandstone cube. Furthermore, this decay is observed to take an exponential trend, characteristic of the discharge of a capacitor. The slow decay of induced potentials may be indicative of lack of saturation in the rock matrix.

High Temperature – Steam Saturated

It is clear that the temporal streaming potential response for this test (Figure 7) is influenced by many mechanisms. At the simplest level, qualitative interpretation reveals that time variations in streaming potentials are a good indicator of changes in sample conditions, more specifically, injection, flow, and pore pressure conditions. For a quantitative interpretation of the data we have attempted to retrieve coupling coefficient information from the increasing pressure and potential area following the start of injection. This methodology has been proven to be an effective way of obtaining coupling coefficients, as demonstrated by the Berea sandstone core sample tests. Relating the pressure and observed potential in this region reveals a coupling coefficient of about 10 mV/atm. This information, however, cannot completely describe the observed response, and it is clear that future testing must be performed to investigate the other mechanisms contributing the streaming potential response. Such mechanisms may include the effect of injectate flashing to steam, the movement of 2 phase fluid/gas through a sand and rock matrix,

thermoelectric self potentials, and sample resistivity changes at high temperature.

For this test we observed large potential drops for all sample faces other than that to which water was flowing towards. That is, water flowing towards the *east* face was mimicked in the streaming potential response by an increase in potential, where as all other side faces showed a potential drop of around 225 mV. We attribute this observation to a combination of factors. First, we propose that current induced in the sand-filled flow pipe is entering the rock via the conducting rock walls of the flow pipe. Therefore, the potential observed on these side faces of the block may be an indicator of that portion of current that is entering the rock matrix. Furthermore, the sample at high temperature will have a lower resistivity, and thus, more current may enter the rock matrix than at low temperatures. Second, we note that a thermoelectric self potential may cause a potential difference on *non-flow* side faces. This type of self-potential is created by the temperature gradient from the center of the sample radial outwards, and in this experiment could be significant resulting from a large temperature gradient (Corwin and Hoover, 1979). These effects may act in opposition to the strong positive electrokinetic response observed on the *east* face of the sample, producing a complex self potential temporal response.

Small-Scale Core Testing – Berea Sandstone

We were able to retrieve coupling coefficients from the injection pump tests at varying pressures by overlaying the pressure drop and streaming potential curves, and then by adjusting their respective axes limits. The coupling coefficient was determined directly from the resulting plot by dividing any potential grid line by the corresponding pressure value. In this way we effectively average hundreds of potential/pressure combinations to determine the coupling coefficient.

This testing program revealed close temporal correlation between the induced pressure drop across the sample and the observed streaming potential. In general, streaming potentials responded well to both increasing and decreasing head. As per the earlier discussion on capacitive effects resulting from incomplete saturation, we are confident that the samples used in these tests were well saturated.

For the streaming potential test of only coarse quartz sand, the coupling coefficient was observed to decrease with increasing pressure drop in a logarithmic fashion, as described by equation 2. This effect has been explained as resulting from flow that is not “fully established” (Reichardt, 1935). That is, for fully established flow the coupling coefficient is constant, as observed in the static head experiments at low pressures. As pressure increases, however, as in the applied pressure experiments, the coupling coefficient decreases.

For the intact core test, the core with hole, and the core with sand-filled hole tests, however, the streaming potential coupling coefficient was found to be constant over a wide range of pressure differences (up to 1.2 MPa). This is in contradiction to experiments by Morgan et al. (1989) and other investigators who observed that the coupling coefficient decreased with increasing pressure drop. We propose that for the empty and sand-filled flow pipe scenario, flow may always be fully established, as the hole diameter is small with respect to the mineral grain diameter.

The coupling coefficient determined for the experiment with a sand-filled hole in the Berea core is the same as that determined for the intact core of Berea sandstone. Furthermore, we observe that the intact core of Berea sandstone and the coarse quartz sand had similar coupling coefficients at low pressures. These coincidental outcomes make it difficult to distinguish the relative effects of each material on the final streaming potential response.

CONCLUSION

Streaming potential experiments on both large-scale 260 mm cubic sandstone samples, and small-scale 25 mm diameter cores show that streaming potentials are a good indicator of flow through a porous medium. Streaming potentials are sensitive to changes in injection parameters and to differences in sample conditions and flow geometry. Large-scale experiments for steam-saturated samples indicate that at high-temperatures the streaming potential response is complex. Future testing will seek to identify the mechanisms contributing to this response. Experiments reveal that incomplete saturation of the sample may induce capacitive effects in the rock matrix leading to a slow exponential decline in observed potentials following the end of injection. Small-scale testing on Berea sandstone cores investigated streaming potential coupling coefficients for different samples including those with conducting boundaries. Coupling coefficients for all testing on Berea sandstone cores were found to be approximately constant over a large range of pressure drop (up to 1.2 MPa), while the coupling coefficient for the coarse quartz sand sample decreased with increasing head. Streaming potentials will be used in future testing to investigate two-phase fluid/gas flow through a porous rock matrix resulting from the injection of cool water into a steam-saturated sample. These results will aide in investigation of the precise mechanisms controlling rock mass damage at injection points in geothermal reservoirs.

REFERENCES

Bogoslovsky, V., and Ogilvy, A. (1970) "Application of Geophysical Methods for Studying the Technical Status of Earth Dams" Geophysical Prospecting, Vol. 18, pp 758-773.

Corwin, R., and Hoover, D. (1979) "The Self-Potential Method in Geothermal Exploration" Geophysics, Vol. 44, pp 226-245.

Johansson, S., Dahlin, T., and Friborg, J. (2000) "Seepage Monitoring by Continuous Measurements of Resistivity and Streaming Potential in Hallby and Sadva Embankment Dams, Sweden" Proc., Commission Internationale des Grand Barrages, Vingtieme Congres des Grands Barrages, Beijing, pp 1099-1123.

Jouniaux, L., Bernard, M., Pozzi, J., and Zamora, M. (2000) "Electrokinetic in Rocks: Laboratory Measurements in Sandstone and Volcanic Samples" Phys. Chem. Earth (A), Vol. 25, No. 4, pp 329-332.

Kawakami, N., et Takasugi, S. (1994) "SP Monitoring During the Hydraulic Fracturing Using the TG-2 Well, Extended Abstracts of Papers" EAGE-56th Meeting & Technical Exhibition, Florence, Italy, I004.

Marquis, G., Darnet, M., and Sailhac, P. (2002) "Monitoring the Electric Potential During the 2000 Hydraulic Stimulation: Results and Perspectives" Document Soultz, IPG Strasbourg, UMR 7516, March.

Morgan, F., Williams, E., and Madden, T. (1989) "Streaming Potential Properties of Westerly Granite with Applications" Journ. Geophys. Res., Vol. 94, No. B9, pp 12,449-12,461.

Ogilvy, A., Ayed, M., and Bogoslovsky, V. (1969) "Geophysical Studies of Water Leakages From Reservoirs" Geophys. Prospect., Vol. 17, pp 36-62.

Overbeek, J. Th. (1952) Colloid Science vol. I, Irreversible Systems, Elsevier, New York.

Reichardt, H. (1935) "Elektrisches Stroemungspotential bei turbulenter stroeming" Phys. Chem. Ser. A, 174, pp 15.

Vichabian, Y., and Morgan, F. (2002) "Self Potentials in Cave Detection" The Leading Edge, September, pp 866-871.

Wurmstich, B., and Morgan, F. (1994) "Modeling of Streaming Potential Responses Caused by Oil Well Pumping" Geophysics, Vol. 59, pp. 46-56.